Available online at www.sciencedirect.com
SCIENCE DIRECT®
ELSEVIER
International Journal of Solids and Structures 42 (2005) 2771–2784
INTERNATIONAL JOURNAL OF SOLIDS and STRUCTURES
www.elsevier.com/locate/ijsolstr

A bending-to-stretching analysis of the blister test in the presence of tensile residual stress

Shu Guo [1], Kai-Tak Wan [2], David A. Dillard *

Engineering Science and Mechanics Department, Virginia Tech, Blacksburg, VA 24061, USA

Received 20 April 2004; received in revised form 6 October 2004
Available online 15 December 2004

Abstract

The adhesion of films and coatings to rigid substrates is often measured using blister geometries, which are loaded either by an applied pressure or a central shaft. The measurement will be affected if there are residual stresses that make a contribution to the energy release rate. This effect is investigated using analytical solutions based on the principle of virtual displacements. A geometrically nonlinear finite element analysis is conducted for comparison. Furthermore, the relationships among strain energy release rate, load, deflection, and fracture radius are discussed in detail. Both analytical solutions and numerical results reveal that uniform tensile residual stresses reduce a specimen's deflection if it experiences plate behavior under small loads. However, this effect becomes negligible when membrane stresses induced by the loading become dominant.

Keywords: Blister test; Thin film; Residual stress; Delamination; Bending; Stretching; Adhesion; Fracture mechanics; Coating

1. Introduction

Blister tests are often used for measuring interfacial fracture energy between a coating film and the substrate (Dannenberg, 1961; Williams, 1969). A thin film bonded to a substrate may be debonded by applying

* Corresponding author. Address: Polymer Division, National Institute of Standards and Technology, 100 Bureau Dr, Mail Stop 8542, Gaithersburg, MD 20899-8542, USA. Tel.: +1 301 975 5732; fax: +1 301 975 4924 (S. Guo), tel.: +1 540 231 4714; fax: +1 540 231 4574 (D.A. Dillard).
E-mail addresses: shu.guo@nist.gov (S. Guo), wankt@umr.edu (K.-T. Wan), dillard@vt.edu (D.A. Dillard).
[1] Currently at: Polymer Division, National Institute of Standards and Technology, 100 Bureau Dr, Mail Stop 8542, Gaithersburg, MD 20899-8542, USA.
[2] Currently at: Department of Mechanical and Aerospace Engineering, University of Missouri-Rolla, Rolla, MO 65409, USA.

0020-7683/$ - see front matter
doi:10.1016/j.ijsolstr.2004.10.007

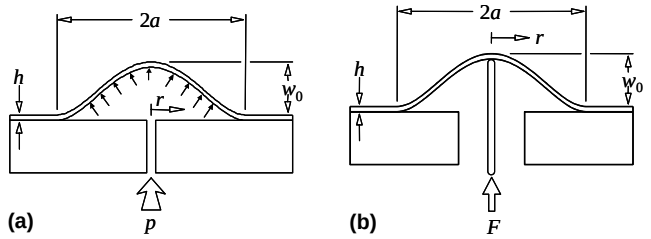

Fig. 1. Schematics of the loading configurations for (a) pressurized blister, (b) shaft-loaded blister (after Wan et al. (2003)).

either a hydrostatic pressure or a central load, as shown in Fig. 1. The deformation mode in a blister film experiences a transition from bending, when subjected to very small loads, to stretching under high loads. In a bending analysis, the in-plane stresses in the specimen are ignored, while bending rigidity is not considered during stretching analysis. A load–deflection curve is linear for a bending plate, but cubic for a stretching membrane. Besides the conventional circular, unconstrained geometry, several alternative blister configurations have been proposed to measure the adhesion energy between thin films and rigid substrates (Chang et al., 1989; Dillard and Bao, 1991; Wan, 2002; Sun et al., 2004). The following review focuses on two standard blister geometries, which will be analyzed in detail later in the paper.

The most conventional blister geometry uses pressure to load a specimen. Bennett et al. (1974) investigated the effect of specimen thickness on the elastic analysis of a pressurized blister, and conducted finite element analysis (FEA) for verification. The analysis of blisters for thin films gained much attention. Hinkley (1983) reported an approximate solution of the pressurized blister without residual stress based on the assumption of a spherical cap for a loaded blister, but gave the wrong solution for the strain energy release rate. Voorthuyzen and Bergveld (1984) solved numerically the von Karman equation for a pressurized blistering film with residual stress. Gent and Lewandowski (1987) later corrected the solution for energy release rate by using a similar method. Allen and Senturia (1988) gave equations for both the load–defection relationship and strain energy release rate for both circular and square specimens with constant residual stress. Lin and Senturia (1990) and Sizemore et al. (1995) experimentally verified their elastic model for thin flexible film and applied a perturbation of bending moment for thick films. Small and Nix (1992) conducted finite element analysis to compare the accuracy of the analytical solutions based on different deflection profiles. Cotterell and Chen (1997) studied the transition from bending to stretching of a blister geometry using Hencky's series solution, and gave a polynomial expression for the strain energy release rate. Using the assumption of a uniform and isotropic membrane stress, Arjun and Wan (2005) gave an approximate analytical solution for a pressurized blister without residual stress, and demonstrated the transition from bending to stretching with increasing load. Recently, still based on the assumption of uniform and isotropic in-pane stresses, Wan et al. (2003) obtained an approximate analytical solution for a clamped circular film in the presence of uniform residual tension (Arjun and Wan, 2005). Jensen and Thouless (1993) analyzed both tensile and compressive residual stresses in a blister specimen for both small linear displacement limit (pure bending) and large nonlinear membrane-type limit (pure stretching). Sheplak and Dugundji (1998) investigated the transition from bending to stretching of a circular plate's deflection with initial stretching using a finite difference technique, and found that tensile residual stress delayed the transition from bending to stretching.

An alternate way of applying load to a blister is by using a rigid shaft to displace the center of the debonding film. Malyshev and Salganik (1965) studied the response of a penny-shape debond by treating the coating as a bending plate. Jensen (1991) and Thouless and Jensen (1994) reported strain energy release rates for a point loaded blister with and without residual stress. Williams (1997) reviewed the strain energy release rate of peel and blister test for flexible films under both applied pressure and a point load. Wan and

Mai (1995), Wan and Liao (1999) and Wan (1999) measured the adhesion energy between a polymer thin film and rigid substrates using the shaft-loaded blister, and developed an approximate analytical solution for the point loaded blister using the assumption of uniform and isotropic in-plane stress. This solution was extended to the case with residual stresses (Wan et al., 2003). During a blister test, the interface is subjected very high level stresses and undergoes inhomogeneous deformations. Large amounts of plastic deformation may result and dominate the behavior during the test. Some researchers have worked on the elastic-to-plastic deformation in blister tests (Thouless, 1994; Margaritis et al., 1994; Wan and Mai, 1995). This topic is beyond the scope of this paper, so we will not discuss about it in this paper.

Although the blister geometry has been investigated intensively, less effort has been devoted to the transition behavior from bending to stretching. Most work emphasized either of the two limits. Furthermore, the effect of tensile residual stress on this transition has obtained less attention.

In this paper, the strain energy release rate, $\mathcal{G}$, was derived for a circular blister debonded from a rigid substrate in the presence of uniform tensile residual stresses. The blister is subjected to either a uniform pressure or a central point load. The relationships among $\mathcal{G}$, load, deflection and debond radius are discussed. Furthermore, a geometrically nonlinear FEA is conducted to verify the analytical solutions, and the discrepancy between analytical solutions and numerical results is investigated.

2. Analytical solution

Wan et al. (2003) reported the solutions for a circular plate stretched by an equal-biaxial membrane stress $N_0 = \sigma_0 t$, where σ_0 is the tensile residual stress in film, and t is the film thickness. The plate is subjected to various loading conditions. Three assumptions were adopted for the analysis: (i) the resultant membrane stress, $N = N_m + N_0$, where N_m is the membrane stress caused by applied loading, is constant over the film area; (ii) the membrane stress is equal-biaxial, i.e. the radial and tangential stresses are equal, $N_r = N_t = N$; and (iii) a small angle approximation is assumed, such that the gradient of the profile is small. For convenience, a few useful non-dimensional parameters are defined as:

$$\beta_m = \left(\frac{N_m a^2}{D}\right)^{1/2}, \quad \beta_0 = \left(\frac{N_0 a^2}{D}\right)^{1/2}, \quad \beta = \left(\frac{(N_m + N_0) a^2}{D}\right)^{1/2}, \quad \rho = \frac{p a^4}{2Dh}, \quad \varphi = \frac{F a^2}{2\pi D h}, \quad W_0 = \frac{w_0}{h}$$

$$\chi = \frac{\mathcal{G}}{pV/A} = \frac{\mathcal{G}}{Fw_0/A}$$

where $D = Eh^3/[12(1-\nu^2)]$ is the flexural rigidity of plate, E is Young's modulus, h is the plate thickness, ν is Poisson's ratio of the plate, V is the blister volume, $A = \pi a^2$ is the debonded area, a is the blister radius and $\mathcal{G}$ is the strain energy release rate during debonding.

For simplicity, the relationship between pressure, p, or central point load, F, and central deflection, w_0, can be expressed in a general form: $F \propto a^{-2} w_0^n$ for the central point loaded blister and $p \propto a^{-4} w_0^n$ for the pressurized case throughout the entire loading region. Here n can be determined from p or F, and w_0. Depending on the degree of deformation, n ranges from 1 to 3 as the dominant response goes from bending to stretching.

2.1. Pressurized blister

The curves of φ and ρ as a function of W_0 for different β_0 at the two limits are shown in Fig. 2(a). The influence of β_0 is important only in the bending and bending-to-stretching regimes. β_0 delays the transition from bending to stretching, but all the curves converge at the stretching limit.

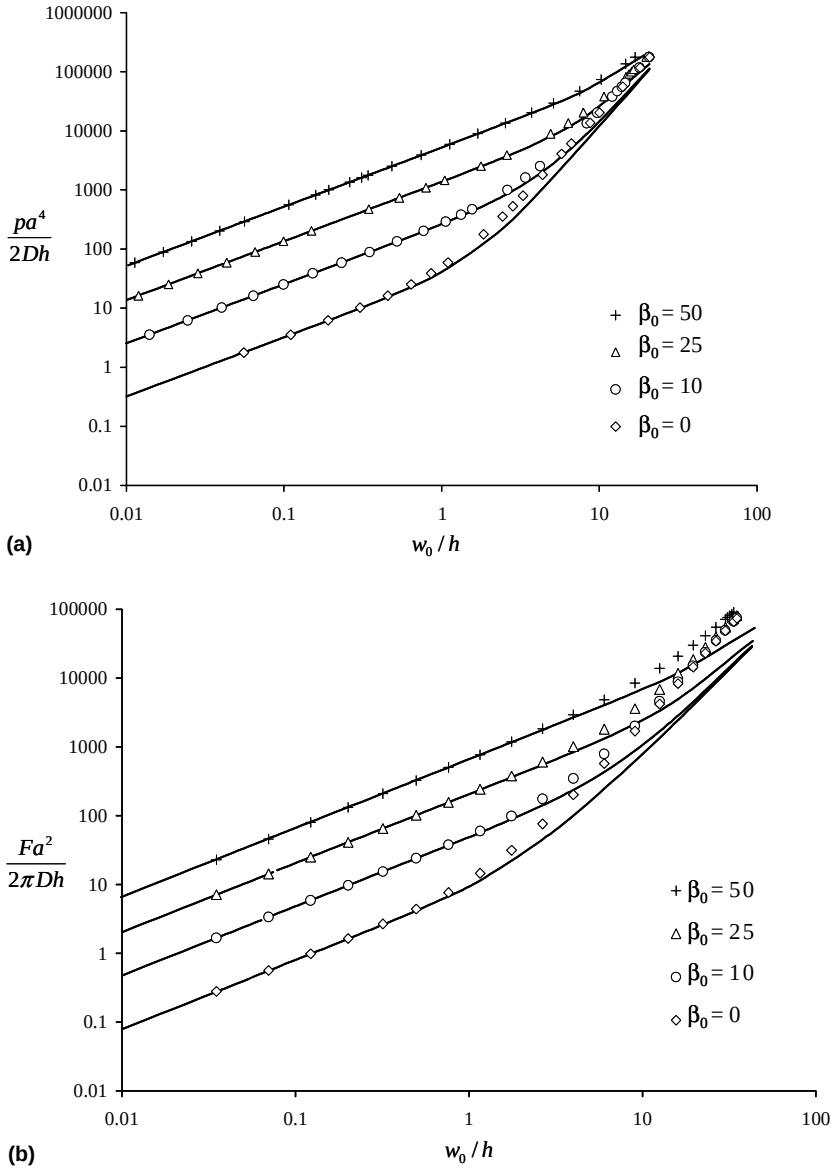

Fig. 2. Constitutive relations for the two blister geometries. Analytical solutions from Wan et al. (2003) are shown as lines and FEA as data points: (a) pressurized blister, (b) central point loaded blister.

Wan and Lim (1998) showed that $\chi = (n+2)/(n+1)$ for a pressurized blister without residual stress, thus $1.25 \leqslant \chi \leqslant 1.5$. The lower bound corresponds to a pure stretching mode ($n = 3$), while the upper bound to pure bending ($n = 1$). An explicit expression of χ at the limit of bending region can be obtained by ignoring the membrane stress caused by external loading, i.e. $\beta = \beta_0$ where β is the total dimensionless membrane stress. Similarly, χ at the membrane limit can also be derived by ignoring β_0, i.e. $\beta = \beta_m$. However, in the transition zone, χ cannot be expressed explicitly. When either the external pressure or the central deflection exceeds a critical threshold, delamination may be driven along the film–substrate interface, or in

some situations, fracture can proceed into either the film or the substrate. For the purpose of this paper, we assume that debonding occurs at or very near the interface. The value of the fracture energy depends on the strain energy release rate (SERR), $\mathcal{G}$, which for a fixed pressure p, can be defined as

$$\mathcal{G} = \frac{\mathrm{d}}{\mathrm{d}A}(U_p - U_e)\bigg|_p \tag{1}$$

where the potential energy

$$U_p = pV \tag{2}$$

and the elastic energy stored in the elastic medium

$$U_e = \int_0^V p\,\mathrm{d}V = \left(\frac{1}{n+1}\right)pV \tag{3}$$

for an elastic film with $p \propto a^{-4}w_0^n$ and $V \propto a^2 w_0$. Substituting (2) and (3) into (1) and assuming a constant n,

$$\mathcal{G} = \left(\frac{n}{n+1}\right)p\frac{\mathrm{d}V}{\mathrm{d}A} \tag{4}$$

thus

$$\chi = \left(\frac{n}{n+1}\right)\left(\frac{a}{2V}\right)\frac{\mathrm{d}V}{\mathrm{d}a} \tag{5}$$

In terms of the already defined variables, (5) can also be written as

$$\chi = \frac{n}{n+1}\frac{\beta_0}{2V}\frac{\mathrm{d}V}{\mathrm{d}\beta_0} \tag{6}$$

The blister volume V can be obtained from integration and expressed simply as $V = k_2\pi a^2 w_0$, where k_2 varies from 1/3 to 1/2, depending on the type of film deformation. If $\rho = k_1(w_0/h)^n$, where k_1 is a function of membrane stress β_m, and can be expressed from the solutions of ρ and W_0 as reported in (Wan et al., 2003). Therefore, V can be rewritten as

$$V = \left\{\left[\frac{p}{2Dh}\left(\frac{D}{N_0}\right)^2\right]^{1/n}\frac{Dh}{N_0}\right\}\left(\frac{V}{a^2h}\frac{1}{\rho^{1/n}}\right)\beta_0^{\frac{2n+4}{n}} \tag{7}$$

The variables in curly brackets are constants independent of a. Substituting (7) into (6), χ can be found as an explicit function of β_m.

2.2. Central point-loaded blister

Following the procedure for $\mathcal{G}$ derivation in the preceding subsection, the normalized strain energy release rate for the point loaded case, χ, can be found to be

$$\chi = \left(\frac{n}{n+1}\right)\left(\frac{a}{2W_0}\right)\frac{\mathrm{d}W_0}{\mathrm{d}a} \tag{8}$$

In terms of the already defined variables, (8) can also be rewritten as

$$\chi = \left(\frac{n}{n+1}\right)\left(\frac{\beta_\mathrm{r}}{2W_0}\right)\frac{\mathrm{d}W_0}{\mathrm{d}\beta_\mathrm{r}} \tag{9}$$

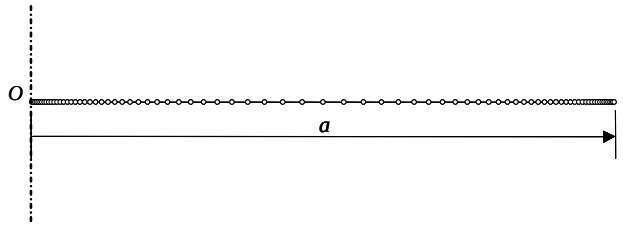

Fig. 3. Axisymmetric shell element mesh used in the finite element analysis.

If dimensionless load φ can be written as $k(W_0)^n$, where k is a function of membrane stress β_m, and can be expressed from the solutions of ρ and W_0 in Wan et al. (2003). Using the definition of φ and W_0 in (Wan et al., 2003), W_0 may be rewritten as

$$W_0 = \left\{ \left(\frac{F}{2\pi Dh} \right) \left(\frac{D}{N_0} \right)^{1/2} \right\}^{1/n} \left(\frac{W_0}{\varphi^{1/n}} \right) \beta_0^{2/n} \tag{10}$$

The variables in the curly brackets are constants independent of a. Substituting (10) into (9), χ then can be found as an explicit function of β_m using a mathematics software such as MATHEMATICA™, [3] though the lengthy solution is not given here. The full solution covers a number of pages in the MATHEMATICA codes.

3. Finite element analysis

In order to verify the preceding analytical solutions, a geometrically nonlinear finite element analysis (FEA) was conducted using the commercial general FEA package ABAQUS®. [4] Axisymmetric quadratic shell elements were adopted to model the film under different loading configurations. Biased meshes were constructed at both the inner and outer boundaries of the membrane, using a length ratio between adjacent elements of 1.25. A blister with a radius of 25 mm and thickness of 0.1 mm was modeled in the numerical simulation. A Young's modulus of 4 GPa and Poisson's ratio of 0.35 was used to mimic a typical filled polymeric material. Equal-biaxial prescribed tensile stresses were applied to the model to simulate the uniform residual stresses. Fig. 3 shows the meshes used for the two loading configurations. Results from the finite element analysis have been shown in Fig. 2(a) and (b) to allow comparisons with the respective analytical solutions.

The strain energy release rate during a blister's delamination from a rigid substrate is determined using the commonly adopted virtual crack closure technique (VCCT) (Rybicki and Kanninen, 1977; Raju, 1987). This method was based on Irwin's theory on fracture (Irwin, 1958) if a crack extends by a small amount Δc, the energy released in the process is equal to that required to close the crack to its original length. Applying VCCT to axisymmetric shell elements, the SERR components can be expressed as:

$$\mathcal{G} = \frac{1}{2\Delta c}(Z_1 w_2 + R_1 u_2 + M_1 \theta_2) \tag{11}$$

where R, Z and M are the reaction forces and moment at the blister edge, u and w are the nodal displacement components along r and z directions respectively, θ is the rotation angle, and the subscripts denote the corresponding nodes, all as shown in Fig. 4.

[3] MATHEMATICA is a mathematics software developed by Wolfram Research, Inc.
[4] ABAQUS is a commercial FEA package developed by ABAQUS, Inc.

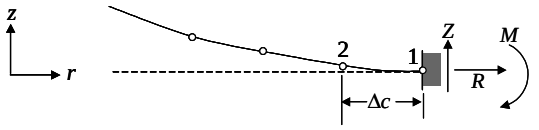

Fig. 4. Schematic of crack front in axisymmetric blister using shell element. Dotted line represents the position of the interface.

4. Discussion

4.1. Relationship between strain energy release rate and central deflection

Fig. 5 shows the curves indicating the relationship between the non-dimensional strain energy release rate, χ, and non-dimensional central deflection $W_0 = w_0/h$. The normalized residual stress β_0 varies from zero to 50. Generally, β_0 tends to reduce the value of χ when W_0 is small, corresponding to bending response, but all the curves for different β_0 continuously converge to the same χ value ($\chi_{\text{stretching}} = 1.25$ for a pressurized blister, and $\chi_{\text{stretching}} = 0.25$ for the point loaded case) when W_0 is significantly large so that stretching in the plate is dominant. When β_0 is sufficiently large (>50) and W_0 is sufficiently small (<0.1), χ reaches constant asymptotic values for the two loading cases (1 for pressurized case and 0 for point loaded situation, respectively) independent of β_0 even at low W_0 limits. The degree of the agreement between the analytical solutions and FEA results is different for the two loading conditions. For pressurized case, analytical solutions agree with FEA data almost perfectly throughout entire loading range. As to pointed loaded situation, notable discrepancy between analytical solutions and FEA results was observed near the stretching limit, though they agree with each other very well at the bending end where W_0 is small. As discussed in Wan et al. (2003) the assumption of equal-biaxial membrane stresses holds reasonably well for the pressurized blister case, but is only a first approximation for pointed loaded configuration if loads are large.

In the following discussions, the relationships between load, central deflection, and blister radius during debonding are discussed. The following non-dimensional parameters are defined to facilitate the discussion:

Non-dimensional fracture toughness: $\Gamma = \frac{\mathcal{G}}{D/h^2}$
Non-dimensional pressure: $\Pi = \frac{p}{D/h^3}$
Non-dimensional point load: $\Phi = \frac{F}{D/h}$
Non-dimensional blister radius: $\alpha = a/h$

Γ is around the range of 0.01 if using the material properties and specimen dimensions used for the FEA analysis and taking $\mathcal{G} = 100\ \text{J/m}^2$ to represent a typical interfacial fracture toughness between a polymeric film and silicon substrate (Hohlfel et al., 1997). Therefore, $\Gamma = 0.01$ is chosen in the following discussions to simulate the typical polymeric thin film system. Because the expressions of the solution based on the uniform and isotropic membrane stress are so complicated that symbolic algebra seems too difficult to operate, Only the FEA results are discussed in the following.

4.2. Relationship between critical central deflection and debond radius

Fig. 6 shows the central deflection W_0 as a function of debond radius α at constant $\Gamma = 0.01$. β_0 ranges from 0 to 50. This figure physically illustrates how central deflections changes with debond radius during blister experiments. It can be seen from the figures that $W_0 \propto a^m$ with $1 \leqslant m \leqslant 2$. In the bending dominant region (small w_0), $m = 2$ and in the stretching dominant region (large w_0), $m = 1$. The mixed bending and stretching transition possesses an intermediate m value.

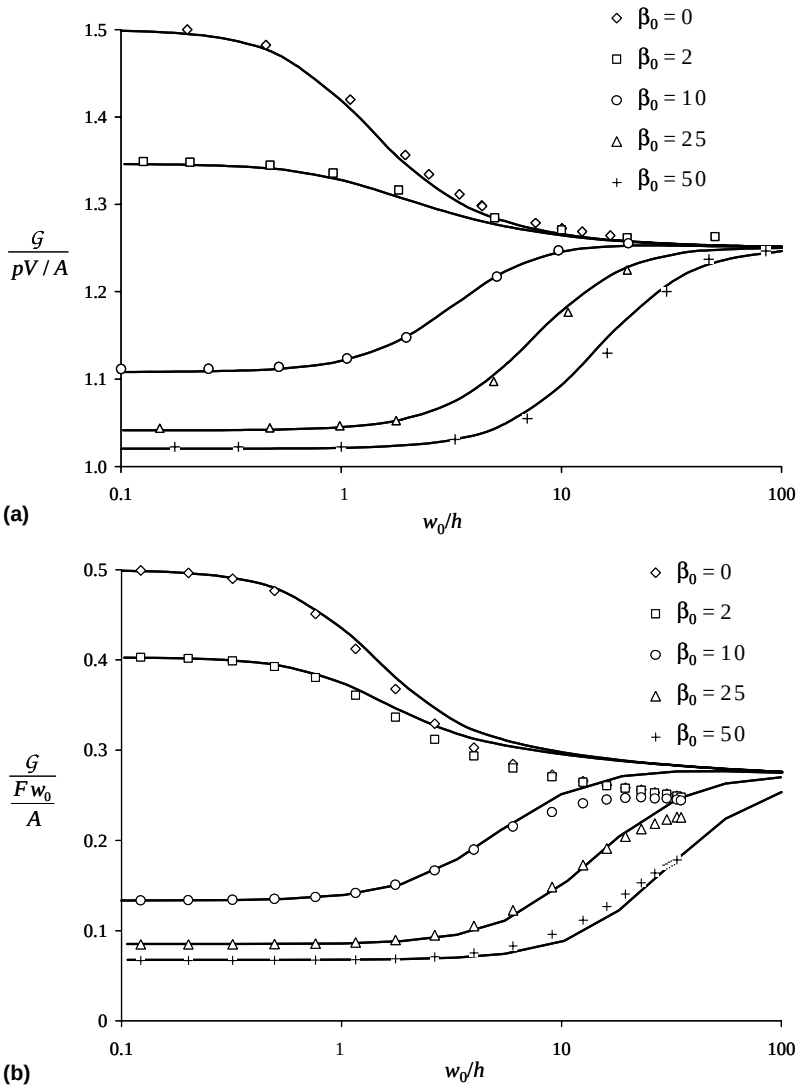

Fig. 5. Normalized strain energy release rate as a function of central deflection W_0: (a) pressurized blister, (b) central point loaded blister.

4.3. Relationship between applied pressure/load and debond radius

Another blister test procedure requires debonding load and fracture radius for fracture energy measurement. Φ and Π as functions of α are illustrated in Fig. 7 for $\Gamma = 0.01$.

For the pressurized blister (Fig. 7(a)), $\Pi \propto \alpha^q$ with $-2 \leqslant q \leqslant -1$. In the bending dominant region (small a), $q = -2$ and in the stretching dominant region (large a), $q = -1$. The mixed bending-to-stretching transition is a function of β_0 and possesses an intermediate q value. The tensile residual stress delays the transition from bending to stretching. Note that $(d\Pi/d\alpha)$ is negative in the entire range of α such that the delamination process is always unstable. Once equilibrium is reached, a small increase in applied pressure or load will lead to a spontaneous catastrophic delamination.

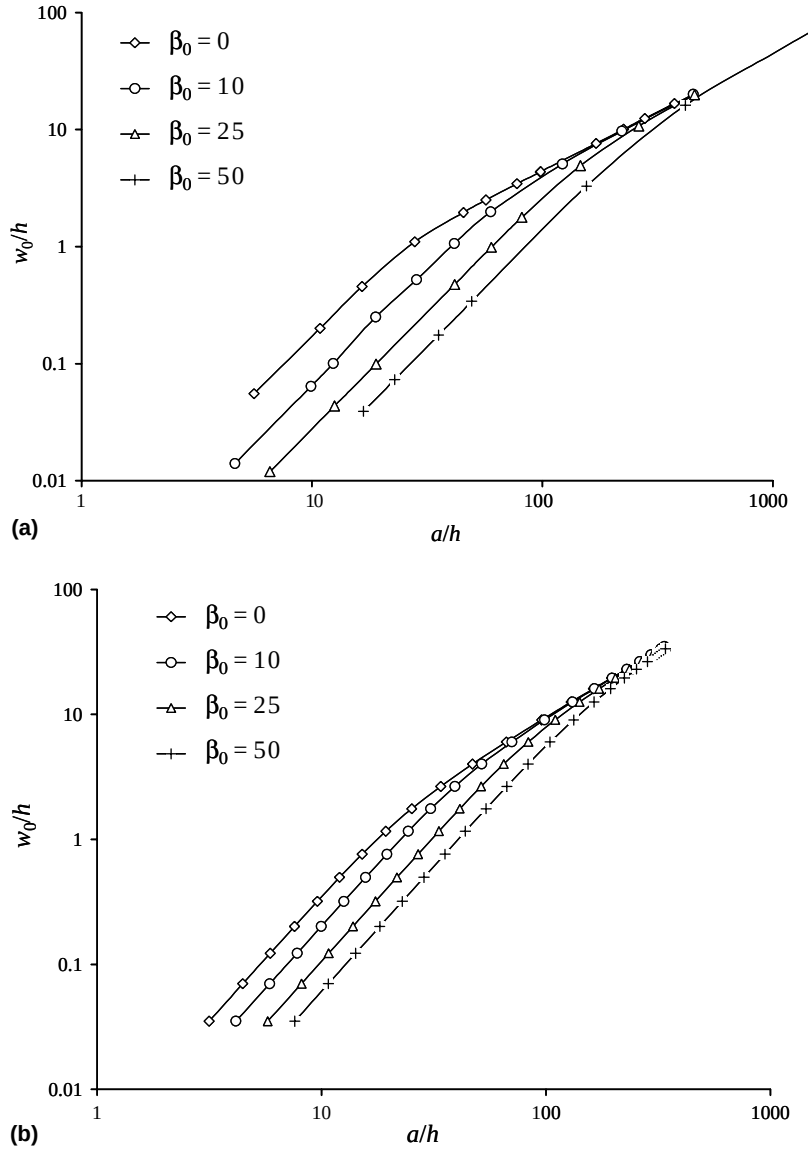

Fig. 6. Central deflection as a function of blister radius during debonding. Data points and lines are FEA results: (a) pressurized blister, (b) central point loaded blister.

For the central point loaded blister (Fig. 7(b)), $\Phi \propto \alpha^r$ with $0 \leqslant r \leqslant 1$. In the bending dominant region (small a), $r = 0$ such that Φ is a constant independent of α and solely depends on β_0 as shown. Since $(d\Phi/d\alpha) = 0$ in this region, the delamination is in a neutral equilibrium, i.e. delamination continues to grow at a constant applied load (Wan and Mai, 1995). The film's response gradually turns into membrane stretching as α increases. Here Φ becomes linear with α and $r = 1$ (Williams, 1997). Note that the delamination process is stable in the stretching dominant range because $(d\Phi/d\alpha) > 0$. All the curves with different β_0 approach the same asymptote at large α. A film delaminating in a neutral equilibrium fashion at small a will eventually come to a halt once the linear $\Phi(\alpha)$ branch is reached.

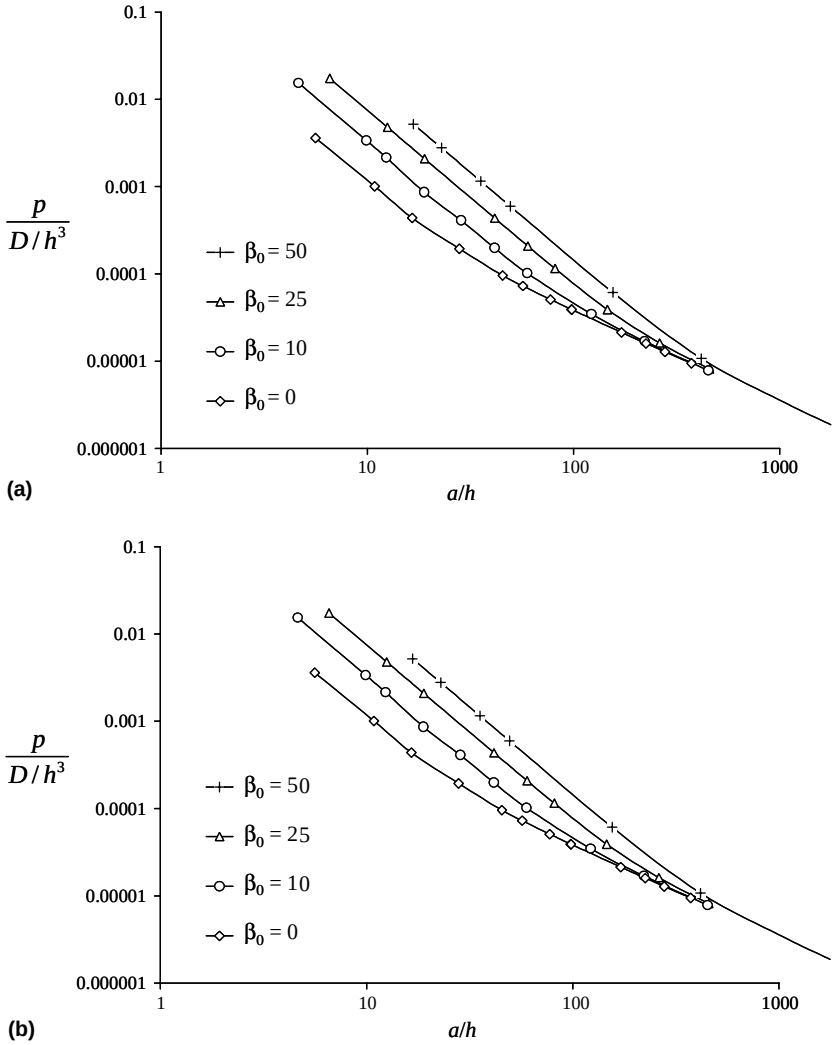

Fig. 7. Applied load as a function of blister radius during debonding: (a) pressurized blister, (b) central point loaded blister.

4.4. Relationship between debonding load and displacement

The compliance of a specimen during fracture tests is often used for $\mathcal{G}$ measurement, thus an understanding of how load changes with displacement is important. Fig. 8 illustrates the non-dimensional pressure or point load as functions of central deflection in the presence of tensile residual stresses.

For the pressurized blister (Fig. 8(a)), no difference is observed between the relationship between Π and W_0 throughout the bending and stretching regions, and can be approximately expressed as $\Pi \propto W_0^{-1}$. This is in consistent with our earlier prediction such that $(\Gamma/\Pi W_0) = 0.5$ in the bending dominant region and $(\Gamma/\Pi W_0) = 5/8$ in the stretching dominant region (Arjun and Wan, 2005).

For the central point loaded blister, $\Phi \propto W_0^b$ with $0 \leqslant b \leqslant 1$, similar to the behavior of $\Phi(\alpha)$ (c.f. Fig. 8(b)). In the bending dominant region (small W_0), $b = 0$ such that Φ is a constant independent of α and solely depends on β_0 as shown. The film's response gradually turns into membrane stretching as W_0

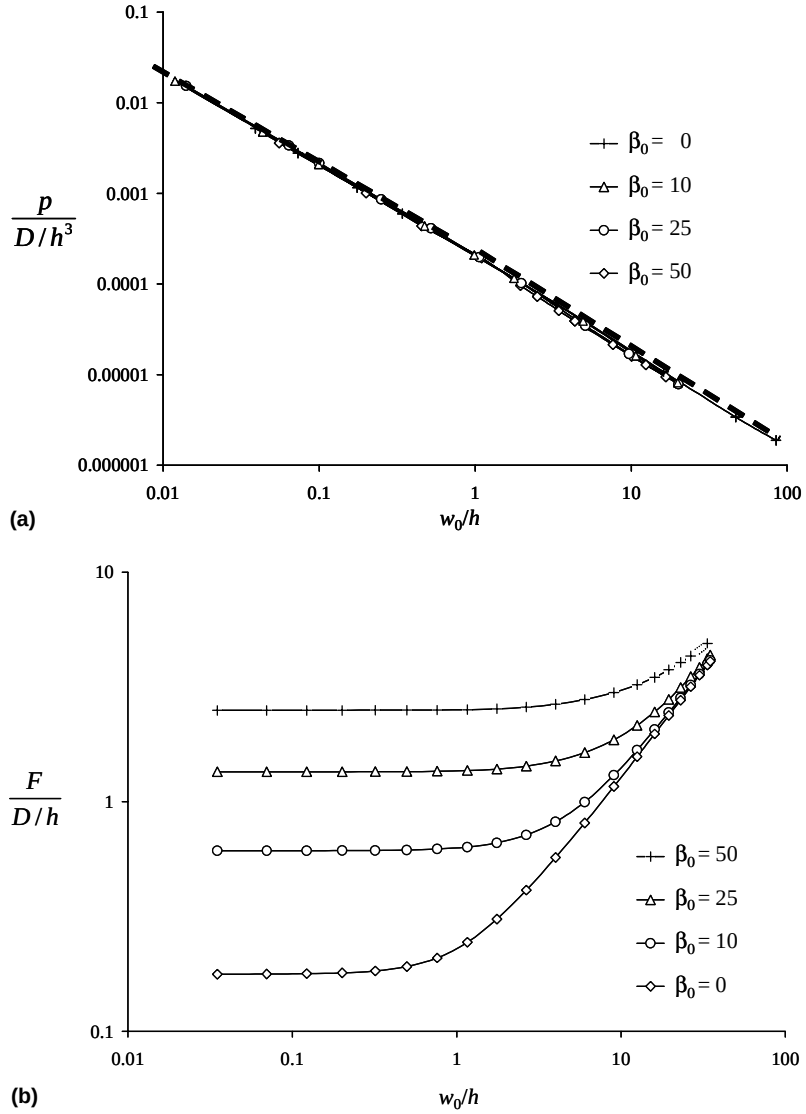

Fig. 8. Applied load as a function of central deflection during debonding: (a) pressurized blister, (b) central point loaded blister.

increases. Here $\Phi(W_0)$ becomes linear with $b = 1$. All the curves with different β_0 approach the same asymptote at large W_0.

4.5. Comparison with other solutions

Pressurized blisters have received many researchers' attention for a long time, and many solutions have been reported, some of which are explicit polynomial expressions. Therefore, it is instructive to compare those solutions with what was reported in this paper. Table 1 lists these solutions for comparison, and Fig. 9 shows ρ versus W_0 relationships from different solutions and FEA results. Solutions of Allen and Senturia (1988) and Sizemore et al. (1995) are correct only for membrane films if residual stress is

Table 1
Comparison of the solutions for pressurized blister geometry[a]

Authors	ρ	$\mathcal{G}/(pV/A)$
Gent and Lewandowski (1987)[b]	$18.82W_0^3$	1.125
Allen and Senturia (1988)	$20.8W_0^3 + 2\beta_0^2 W_0$	$\frac{15W_0^2+1.15\beta_0^2}{12W_0^2+1.15\beta_0^2}$
Lin and Senturia (1990)	$32W_0 + 21.88W_0^3 + 2\beta_0^2 W_0$	Not provided
Sizemore et al. (1995)	$19.6W_0^3 + 2\beta_0^2 W_0$	$\frac{359W_0^4+42.4W_0^2\beta_0^2+\beta_0^4}{28.7W_0^4+39.1W_0^2\beta_0^2+\beta_0^4}$
Williams (1997)	Not provided	$\frac{15W_0^2+1.15\beta_0^2}{12W_0^2+1.15\beta_0^2}$

[a] Poisson's ratio $v = 0.3$ for calculation.
[b] Residual stress is not considered.

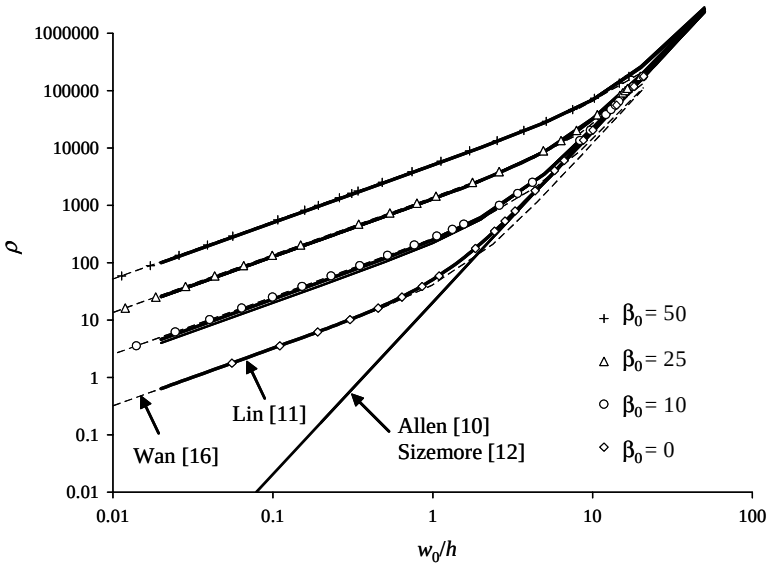

Fig. 9. Constitutive relations for the pressurized blister geometry from different solutions listed in Table 1. Data points are FEA results as comparison. The lines for non-zero β_0 from Allen and Senturia (1988), Sizemore et al. (1995) and Lin and Senturia (1990) superposed with FEA results.

not present. For the cases with residual stresses, however, they show encouraging agreement with FEA models. The solution proposed in this chapter can capture the response from bending to stretching, thus is more complete.

Fig. 10 shows χ versus W_0 for a pressurized blister. As to the $\mathcal{G}$ calculation, only three explicit solutions were found and significantly different shapes were observed for different solutions, although they agree with each other in the stretching limit. The three solutions predict different values at the bending limit, and two of them deviate from FEA results. All solutions indicate that uniform tensile residual stresses delay the transition from bending to stretching. But, FEA results reveal that residual stress also changes the behavior in the bending-controlled domain, thus, attention should be given when such solutions are applied to practice. There is a good agreement between Wan's model and FEA.

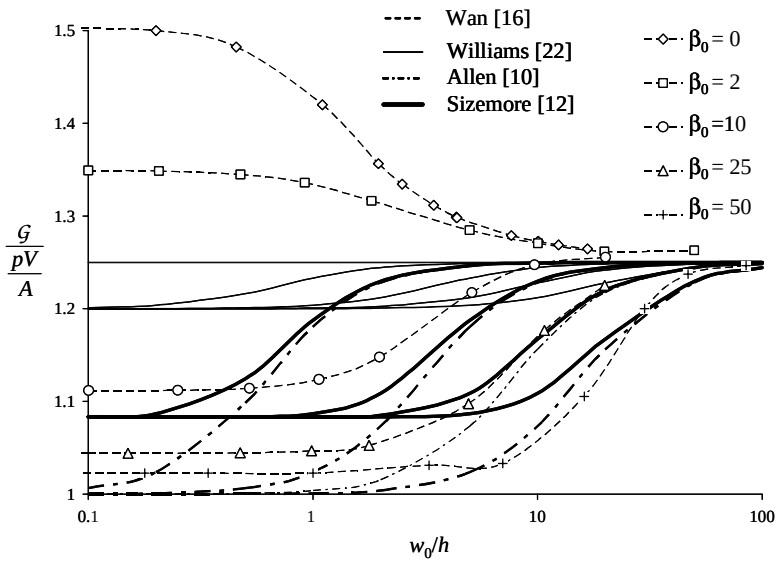

Fig. 10. Normalized strain energy release rate as a function of central deflection W_0 from the solutions listed in Table 1 for a pressurized blister. FEA results are shown as data points for comparison.

5. Conclusions

The deformation and delamination behavior of a circular blister under both pressure and central point load were investigated over a wide range of transverse loadings and initial in-plane uniform tensile stresses. If the blister is very thin or flexible, the residual stress can be ignored for deflection and $\mathcal{G}$ calculation using either measured load or displacement data. However, when bending or bending-to-stretching transition behavior is significant during the debonding process, the residual stress must be taken into account, and the correct equations should be adopted to measure the adhesion energy. The results reported in this paper will be useful to the engineers intending to measure residual stresses of thin films, and also for characterizing the adhesion energy between a thin film and rigid substrate using one of the two geometries.

Acknowledgements

This work was funded in part by the Hewlett Packard Corporation. We would like to acknowledge the Center of Adhesive and Sealant Science (CASS) of Virginia Tech for fostering interdisciplinary research in adhesion science, and the Department of Engineering Science and Mechanics for providing facilities and support. We are grateful to Dr. Paul Reboa of the Hewlett Packard Corporation for helpful discussions.

References

Allen, M.G., Senturia, S.D., 1988. Analysis of critical debonding pressures of stressed thin films in the blister test. Journal of Adhesion 25, 303–315.

Arjun, A., Wan, K.-T., 2005. Derivation of the strain energy release rate G from first principles for the pressurized blister test. International Journal of Adhesion and Adhesives 25, 13–18.

Bennett, S.J., Devries, K.L., Williams, M.L., 1974. Adhesive fracture mechanics. International Journal of Fracture 10, 33–43.

Chang, Y.S., Lai, Y.H., Dillard, D.A., 1989. The constrained blister—a nearly constant strain energy release rate test for adhesives. Journal of Adhesion 27, 197–211.

Cotterell, B., Chen, Z., 1997. The blister test—transition from plate to membrane behavior for an elastic material. International Journal of Fracture 86, 191–198.

Dannenberg, H., 1961. Measurement of adhesion by a blister method. Journal of Applied Polymer Science 5, 125–134.

Dillard, D.A., Bao, Y., 1991. The peninsula blister test: a high and constant strain energy release rate fracture specimen for adhesives. Journal of Adhesion 33, 253–271.

Gent, A.N., Lewandowski, L.H., 1987. Blow-off pressure for adhering layers. Journal of Applied Polymer Science 33, 1567–1577.

Hinkley, J.A., 1983. A blister test for adhesion of polymer films to SiO_2. Journal of Adhesion 16, 115–126.

Hohlfel, R.J., Luo, H., Vlasska, J.J., Chidsey, C.E.D., Nix, W.D., 1997. Measuring interfacial fracture toughness with the blister test. Material Research Symposium Proceedings 436, 115–120.

Irwin, G.R., 1958. Fracture. Handbuch der Physik 6, 551.

Jensen, H.M., 1991. The blister test for interfacial toughness measurement. Engineering Fracture Mechanics 40, 475–486.

Jensen, H.M., Thouless, M.D., 1993. Effects of residual stresses in the blister test. International Journal of Solids and Structures 30, 779–795.

Lin, P., Senturia, S.D., 1990. The in situ measurement of biaxial modulus and residual stress of multi-layer polymeric thin films. Materials Research Society Symposium Proceedings 188, 41–46.

Malyshev, B.M., Salganik, R.L., 1965. The strength of adhesive joints using the theory of cracks. International Journal of Fracture 1, 114–128.

Margaritis, G., Sikorski, S.A., McGarry, F.J., 1994. Elastic–plastic finite element method analysis and application of the island blister test. Journal of Adhesion Science and Technology 8, 273–287.

Raju, I.S., 1987. Calculation of strain-energy release rate with higher order and singular finite elements. Engineering Fracture Mechanics 28, 251–274.

Rybicki, E.F., Kanninen, M.F., 1977. A finite element calculation of stress intensity factors by a modified crack closure integral. Engineering Fracture Mechanics 9, 931–938.

Sheplak, M., Dugundji, J., 1998. Large deflections of clamped circular plates under initial tension and transitions to membrane behavior. ASME Journal of Applied Mechanics 65, 107–115.

Sizemore, J., Hohlfelder, R.J., Vlassak, J.J., Nix, W.D., 1995. Measuring the adhesion of diamond thin films to substrates using the blister test. Materials Research Society Symposium Proceedings 383, 197–207.

Small, M.K., Nix, W.D., 1992. Analysis of the accuracy of the bulge test in determining the mechanical properties of the thin film. Journal of Materials Research 7, 1553–1563.

Sun, Z., Wan, K.-T., Dillard, D.A., 2004. A theoretical and numerical study of thin film delamination using the pull-off test. International Journal of Solids and Structures 41, 717–730.

Thouless, M.D., 1994. Fracture mechanics for thin film adhesion. IBM Journal of Research and Development 38, 367–377.

Thouless, M.D., Jensen, H.M., 1994. The effect of residual stresses on adhesion measurement. Journal of Adhesion Science and Technology 8, 579–586.

Timoshenko, S.P., Woinowsky-Krieger, S., 1959. Theory of Plates and Shells, second ed. McGraw-Hill, New York.

Voorthuyzen, J.A., Bergveld, P., 1984. The influence of tensile forces on the deflection of circular diaphragms in pressure sensors. Sensors and Actuators 6, 201–213.

Wan, K.-T., 1999. Fracture mechanics of a shaft-loaded blister test—transition from a bending plate to a stretching membrane. Journal of Adhesion 70, 209–219.

Wan, K.-T., 2002. Adherence of a axisymmetric flat punch onto a clamped plate-transition from a rigid plate to a flexible membrane. ASME Journal of Applied Mechanics 69, 104–109.

Wan, K.-T., Liao, K., 1999. Measuring mechanical properties of thin flexible films by a shaft-loaded blister test. Thin Solid Films 352, 167–172.

Wan, K.-T., Lim, S.-C., 1998. The bending to stretching transition of a pressurized blister test. International Journal of Fracture 92, L43–L47.

Wan, K.-T., Mai, Y.-W., 1995. Modified blister tests for evaluation of thin flexible membrane adhesion on rigid substrate. Materials Science Research International 1, 78–81, June.

Wan, K.-T., Mai, Y.W., 1995. Fracture mechanics of a shaft-loaded blister of thin flexible membrane on rigid substrate. International Journal of Fracture 74, 181–197.

Wan, K.-T., Horn, R.G., Courmont, S., Lawn, B.R., 1993. Pressurised internal lenticular cracks at healed mica interfaces. Journal of Materials Research 8, 1128–1136.

Wan, K.-T., Guo, S., Dillard, D.A., 2003. A theoretical and numerical study of a thin clamped circular film under an external load in the presence of residual stress. Journal of Solid Thin films 425, 150–162.

Williams, M.L., 1969. The continuum interpretation for fracture and adhesion. Journal of Applied Polymer Science 13, 29–40.

Williams, J.G., 1984. Fracture Mechanics of Polymers. John Wiley & Sons Ltd., London.

Williams, J.G., 1997. Energy release rates for the peeling of flexible membranes and the analysis of blister tests. International Journal of Fracture 87, 265–288.